

# Timoshenko Beam with Uncertainty on the Boundary Conditions

Thiago G. Ritto  
thiagoritto@gmail.com

Rubens Sampaio

Emeritus Member, ABCM  
rsampaio@puc-rio.br

Pontifical Catholic University of Rio de Janeiro –  
PUC-Rio  
Mechanical Engineering Department  
22453-900 Rio de Janeiro, RJ, Brazil

Edson Cataldo

ecataldo@im.uff.br  
Fluminense Federal University - UFF  
Applied Mathematics Department  
Graduate Program in Telecommunications  
Engineering  
24020-140 Niterói, RJ, Brazil

*In mechanical system modeling, uncertainties are present and, to improve the predictability of the models, they should be taken into account. This work discusses uncertainties present in boundary conditions using the model of a vibrating Timoshenko beam, free in one end and pinned with rotation constrained by a linear elastic torsional spring in the other end. The Finite Element Method is used to discretize the system and two probabilistic approaches are considered to model the uncertainties: (1) the stiffness of the torsional spring is taken as uncertain and a random variable is associated to it (parametric probabilistic approach); (2) the whole stiffness matrix is considered as uncertain and a probabilistic model is constructed for the associated random matrix (nonparametric probabilistic approach). In both approaches, the probability density functions are deduced from the Maximum Entropy Principle. In the first approach only the uncertainty of a parameter is taken into account, and in the second approach, the uncertainties of the model are taken into account, globally. Both approaches are compared and their capability to improve the predictability of the system response is discussed.*

**Keywords:** model uncertainty, Timoshenko beam, boundary conditions, stochastic mechanics, parametric probabilistic approach, nonparametric probabilistic approach

## Introduction

Uncertainties have been studied in order to improve the predictability of models. In a general way, uncertainties can be classified in two types: data uncertainties and model uncertainties.

The aim here is to model uncertainties present on the boundary conditions of a beam, considering those two types of uncertainties.

This work has, basically, two main motivations. The first one comes from the fact that, in general, natural frequencies measured from a cantilever beam do not match the natural frequencies predicted from numerical simulation, even if the numerical errors are minimized. The second one is to investigate the nonparametric stochastic approach (which takes into account model uncertainty) for uncertainties on the boundary conditions.

Probability tools are used to model the uncertain boundary conditions, that is, random variables are associated to the uncertain parameters or matrices and probability density functions are constructed. The strategy used here is the same applied by Soize (2001, 2005), Cataldo et al. (2007, 2008, 2009), and Sampaio and Soize (2007).

The process of modeling mechanical systems introduces two types of uncertainties: (1) uncertainties related to the parameters of the model such as geometrical and constitutive parameters, which we call *data uncertainties*, and (2) uncertainties due to the model chosen (beam theory, shell theory, etc.), including boundary conditions, which we call *model uncertainties*.

To discuss uncertainties present on the boundary conditions of a vibrating beam, the model used is a Timoshenko beam free in one end and pinned with rotation constrained by a linear elastic torsional spring in the other end. This model is the one proposed in Ritto et al. (2008) and it shows good agreement with experimental results. The uncertainties analyzed are those related to the torsional spring and, also, related to the stiffness matrix, in the corresponding discretized problem using the Finite Element Method.

First, the torsional spring is considered uncertain and a random variable is associated to it. This randomization process is called the parametric stochastic approach because model uncertainty is not considered (a probability density function is constructed for a parameter of the model). Afterwards, the whole stiffness matrix is considered uncertain. This other randomization process is called the nonparametric stochastic approach because model uncertainty is taken into account (probability density functions are constructed for the matrices used in the model). This second approach was developed by Soize (2001, 2005).

In order to construct a probabilistic model, the necessary probability density functions are constructed based on the Maximum Entropy Principle (Jaynes, 1957a,b) and this strategy considers only the available information to construct the probability density functions. Among all of the possible probability density functions, it is chosen the one with the maximum entropy (or uncertainty). This concept of entropy is the one used by Shannon (1948) and some applications of this method can be found in Kapur and Kesavan (1992).

In order to avoid misunderstandings with deterministic and random variables, the deterministic stiffness is denoted by  $k_i$  and the corresponding random variable is denoted by  $K_i$ . The deterministic stiffness matrix is denoted by  $[K]$ , and the corresponding random matrix is denoted by  $[K]$ . The mean value associated with the random stiffness matrix is represented by  $[\underline{K}]$ .

The organization of this article is as follows: Section 2 presents the mean model, that is, the corresponding deterministic model. Section 3 presents the procedure to build the corresponding stochastic problem, i.e., the stochastic modeling. Section 4 presents the numerical simulations where a stochastic Monte Carlo solver (Rubinstein, 1981) is used to generate the independent realizations of the random variables, and, finally, in Section 5 concluding remarks are outlined.

## Nomenclature

$A$  = cross section area,  $m^2$   
 $conv$  = convergence function

- $det$  = determinant of a matrix
- $E$  = elasticity modulus, Pa
- $\mathbf{f}$  = excitation force vector
- $\hat{\mathbf{f}}$  = force vector in the frequency domain
- $G$  = shear modulus, Pa
- $h$  = Frequency Response Function
- $H$  = random Frequency Response Function
- $I$  = moment of inertia,  $m^4$
- $k_s$  = shear correction factor
- $k_t$  = torsional stiffness, N/m
- $l$  = element size, m
- $L$  = beam length, m
- $n_s$  = number of Monte Carlo simulations
- $p_X$  = probability density function of random variable  $X$
- $T$  = kinetic energy, N.m
- $tr$  = trace of a matrix
- $\mathbf{u}$  = displacement vector
- $\mathbf{U}$  = random displacement vector
- $\hat{\mathbf{u}}$  = displacement vector in the frequency domain
- $\hat{\mathbf{U}}$  = random displacement vector in the frequency domain
- $U$  = potential energy of deformation, N.m
- $[C^{(e)}]$  = element damping matrix
- $[K^{(e)}]$  = element stiffness matrix
- $[M^{(e)}]$  = element mass matrix
- $[C]$  = damping matrix
- $[K]$  = stiffness matrix.
- $[\mathbf{K}]$  = random stiffness matrix
- $[M]$  = mass matrix

**Greek Symbols**

- $\delta$  = dispersion parameter of a probability distribution, or symbol of variation (depending on the context)
- $\rho$  = density,  $kg/m^3$
- $\mathbf{1}_B(x)$  assumes value one if  $x$  belongs to  $B$  and zero otherwise

**Subscripts**

- $a$  axial
- $r$  rotation
- $v$  vertical
- 1 node 1
- 2 node 2
- $K_t$  torsional stiffness
- $[\mathbf{K}]$  stiffness matrix

**Mean Model**

Figure 1 sketches the beam geometry as well the finite element used for the discretization.

In Fig. 1  $k_t$  is the torsional stiffness,  $L$  is the length of the beam,  $h$  and  $b$  are the dimensions of the rectangular cross sectional area, and  $\mathbf{u}^{(e)} = [u_{1a} u_{1v} u_{1r} u_{2a} u_{2v} u_{2r}]^T$  is the displacement of an element.

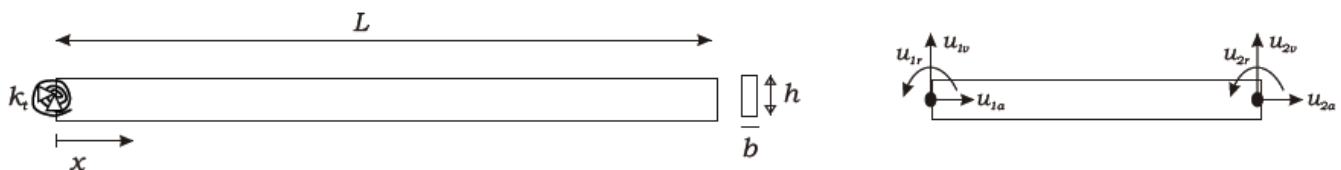


Figure 1. Beam sketch (left) and beam element (right).

Each finite element of the Timoshenko beam model has three degrees of freedom (axial, vertical (or transverse), and rotational) at each node. This model takes shearing into account, and the cross sections remain plane (but not necessarily perpendicular to the neutral axis), as shown in Fig. 2.

The degrees of freedom are: the axial displacement ( $u_a$ ); the vertical displacement ( $u_v$ ); and the rotation ( $u_r$ ). The shear angle is given by

$$\gamma = \frac{\partial u_v}{\partial x} - u_r$$

The variational form of strain energy is given by Eq.(1):

$$\delta U = \int_0^L [\delta u_a (EA u_a') + \delta u_r (EI u_r') + \delta (u_r - u_v') G A k_s (u_r - u_v')] dx + k_t u_r(0, t) \delta u_r(0, t) \tag{1}$$

We denote the derivative with respect to  $x$  by a prime,  $'$ ,  $E$  is the elasticity modulus,  $G$  is the shear modulus,  $k_s$  is the shear correction factor,  $I$  is the moment of inertia,  $L$  is the beam length, and  $A$  is the cross section area. The last term in Eq. (1) is related to the torsional spring in the boundary  $x = 0$ .

The virtual work done by inertial forces are given by Eq. (2):

$$\delta T = \int_0^L \delta u_a (\rho A \ddot{u}_a) + \delta u_v (\rho A \ddot{u}_v) + \delta u_r (\rho I \ddot{u}_r) dx \tag{2}$$

To give more flexibility in applications, damping is taken into account as a Rayleigh damping proportional to the mass,  $[C] = a[M]$ , where  $a$  is a positive constant. Note that if  $a = 0$  there is no damping. It is a standard procedure to construct the element matrices, see for instance Sampaio and Ritto (2008); Inman (2007); Reddy (2005) and the shape functions used for a Timoshenko beam can be found in Nelson (1980); Bazoune and Khulief (2002).

$$[M^{(e)}] = \rho A \frac{1}{420} \begin{bmatrix} 140 & 0 & 0 & 70 & 0 & 0 \\ 0 & 156 & 22l & 0 & 54 & -13l \\ 0 & 22l & 4l^2 & 0 & 13l & -3l^2 \\ 70 & 0 & 0 & 140 & 0 & 0 \\ 0 & 54 & 13l & 0 & 156 & -22l \\ 0 & -13l & -3l^2 & 0 & -22l & 4l^2 \end{bmatrix}; \tag{3}$$

$$[C] = a[M] \tag{3}$$

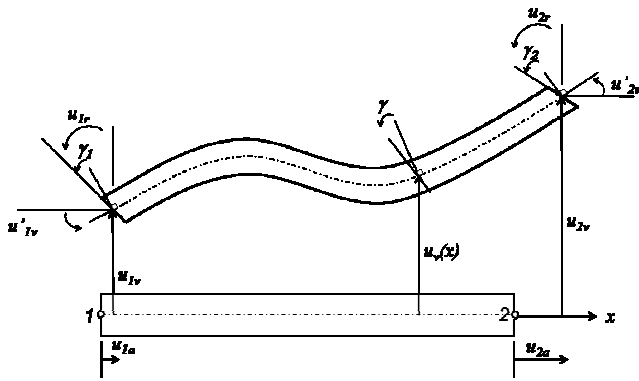


Figure 2. Timoshenko beam model.

$$[K^{(e)}] = \rho \frac{E}{1+m} \begin{bmatrix} A(1+m)/l & 0 & 0 & -A(1+m)/l \\ 0 & 12I/l^3 & 6I/l^2 & 0 \\ 0 & 6I/l^2 & 4I(1+m/4)/l & 0 \\ -A(1+m)/l & 0 & 0 & A(1+m)/l \\ 0 & -12I/l^3 & -6I/l^2 & 0 \\ 0 & 6I/l^2 & 2I(1+m/2)/l & 0 \end{bmatrix}, \quad (4)$$

$$\begin{bmatrix} 0 & 0 \\ -12I/l^3 & 6I/l^2 \\ -6I/l^2 & 2I(1+m/2)/l \\ 0 & 0 \\ 12I/l^3 & -6I/l^2 \\ -6I/l^2 & 4I(1+m/4)/l \end{bmatrix}$$

where

$$m = \left( \frac{12}{l^2} \right) \left( \frac{EI}{GAk_s} \right)$$

and  $l$  is the size of the element.

The essential boundary conditions at  $x = 0$  are given by  $u_a|_{x=0} = 0$  and  $u_v|_{x=0} = 0$  and after assembling the matrices, from the system discretized using the Finite Element Method, Eq. (5) is obtained:

$$[M]\ddot{\mathbf{u}}(t) + [C]\dot{\mathbf{u}}(t) + [K]\mathbf{u}(t) = \mathbf{f}(t), \quad (5)$$

where  $[M]$ ,  $[C]$ , and  $[K]$  are the mass, damping, and stiffness matrices, which are real and positive-definite. The external force is represented by the vector  $\mathbf{f}(t)^T = (f_{1a} f_{1v} f_{1r} f_{2a} f_{2v} f_{2r} \dots f_{nr})$  and the displacements  $(u_{1a} u_{1v} u_{1r} u_{2a} u_{2v} u_{2r} \dots u_{nr})$  are the components of the vector  $\mathbf{u}(t)^T$ .

### Frequency Response Function (FRF) – Mean Model

The resulting linear dynamical system written in the frequency domain is given by Eq. (6) (Ewins, 1984):

$$(-\omega^2[M] + i\omega[C] + [K])\hat{\mathbf{u}}(\omega) = \hat{\mathbf{f}}(\omega) \quad (6)$$

So, the response in the frequency domain is given by Eq. (7):

$$\hat{\mathbf{u}}(\omega) = (-\omega^2[M] + i\omega[C] + [K])^{-1} \hat{\mathbf{f}}(\omega) \quad (7)$$

Let  $\hat{f}_{Lv}$  be the Fourier transform of the force component  $f_{Lv}$  applied at  $x = L$ , and  $\hat{u}_{Lv}$  be the Fourier transform of  $u_{Lv}$ , which is the vertical component of the displacement vector at  $x = L$ . For the cantilever beam, the point  $x = L$  is the most appropriate to observe the response, so we are mostly concerned with the FRF ( $h$ ) defined by Eq. (8):

$$h(\omega) = \frac{\hat{u}_{Lv}(\omega)}{\hat{f}_{Lv}(\omega)} \quad (8)$$

An example is performed considering a homogeneous material and uniform geometry with  $E = 2e11\text{N/m}^2$ ,  $a = 2.5$ ,  $k_t = 10^7\text{N/m}$ ,  $\rho = 7850\text{kg/m}^3$ ,  $\nu = 0.3$ ,  $L = 0.5\text{m}$ ,  $b = 1\text{cm}$ , and  $h = 5\text{cm}$ . The convergence is checked using the Rayleigh coefficient given by Eq. (9):

$$Ray_i = \omega_i^2 = \frac{\phi_i^T [K] \phi_i}{\phi_i^T [M] \phi_i} \quad (9)$$

where  $\omega_i$  is the  $i$ -th natural frequency and  $\phi_i$  is the associated  $i$ -th Normal Mode. For a precision of 99% in the fourth normal mode, it was necessary to construct a mesh of sixteen finite elements. The corresponding FRF is shown in Fig. 3.

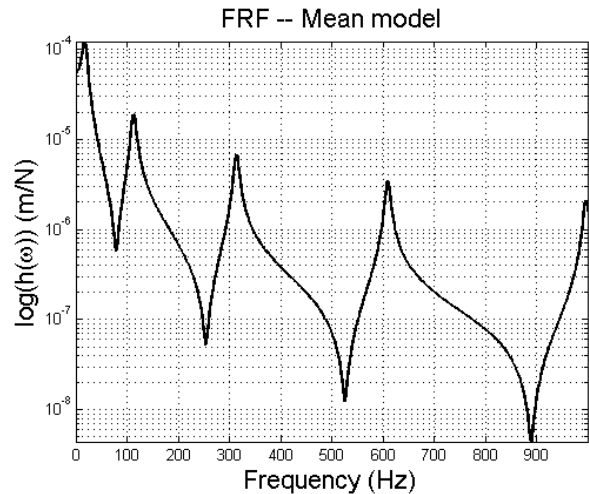


Figure 3. Frequency Response Function.

The finite element approximation of the displacement is computed on frequency band  $B = [0; 1000]$  Hz, and the first four natural frequencies are 18 Hz, 113 Hz, 314 Hz and 609 Hz.

### Stochastic Model

The corresponding stochastic model is constructed choosing parameters and matrices as uncertain and associating random variables to them.

The problem is, then, divided in two cases: (1) a parametric stochastic approach, in which only the stiffness of the torsional spring is chosen as uncertain and a random variable is associated to it, and (2) a nonparametric stochastic approach, in which the whole stiffness matrix is chosen as uncertain and a random matrix is associated to it.

The construction of the probability distributions is crucial in a stochastic analysis and a strategy should be adopted to their construction. Here, it is used some information about the random variables we are sure about. Then, the Maximum Entropy Principle is applied to obtain the distribution that maximizes the uncertainty, given the information we know about the variables. This is a good strategy to be adopted when there are not many experimental data available because we assure the coherence between the realizations of the random variables and the physics of the problem. More examples can be found in Soize (2001), Cataldo et al. (2008).

In both approaches, the deterministic stiffness matrix  $[K]$  is substituted by a random matrix  $[\mathbf{K}]$ , in Eq. (5). However, the construction of the probability density function will change, depending on the approach used. So, we can rewrite Eq. (10) as:

$$[M]\ddot{\mathbf{U}}(t) + [C]\dot{\mathbf{U}}(t) + [\mathbf{K}]\mathbf{U}(t) = \mathbf{f}(t) \tag{10}$$

where  $\mathbf{U}$  is the stochastic process associated with the response of the corresponding stochastic system. Writing Eq. (10) in the frequency domain, we obtain Eq.(11):

$$(-\omega^2 [M] + i\omega [C] + [\mathbf{K}]) \hat{\mathbf{U}}(\omega) = \hat{\mathbf{f}}(\omega) \tag{11}$$

**Probabilistic Model of the Torsional Spring Stiffness**

The first probabilistic approach to be used is the so called parametric stochastic approach, in which the uncertain torsional spring stiffness  $k_t$  is modeled by the random variable  $K_t$ , and an appropriate probabilistic model is constructed. We take for granted that the values of the parameters one wants to randomize are constrained by the physics of the problem. A probabilistic distribution has to be assigned to these possible values. The probability of values that are not admitted is, of course, zero. For example, supposing that the parameter is the rigidity, its values are no positive real number. To assign a normal distribution to the rigidity is, of course, wrong, since this assignment means that the rigidity might be negative. Unfortunately, this is a common mistake.

The strategy used here is based on the Maximum Entropy Principle and the usable information about  $K_t$  are: (1) it is a positive random variable, so its support is  $]0, +\infty[$ ; (2) its expected value is known and it is given by  $E\{K_t\} = \underline{K}_t$ ; and (3)  $E\{1/K_t^2\} < +\infty$ , because the displacement of a spring with random stiffness should be a second order random variable. To understand this last constraint, consider a simple mechanical system model,  $f = ku$ . If the stiffness is random, the displacement is random:  $f = KU$ . Physically,  $U$  must have finite dispersion (must be a second order random variable), i.e.,  $E\{U^2\} < +\infty$ , then  $E\{U^2\} = E\{(f/K)^2\} = f^2 E\{(1/K)^2\} < +\infty$ . So  $E\{1/K^2\} < +\infty$ .

The probability density function of  $K_t$ , using the Maximum Entropy Principle, yields (Soize, 2008):

$$p_{K_t}(k_t) = 1_{]0, +\infty[}(k_t) \frac{1}{\underline{K}_t} \left(\frac{1}{\delta_{K_t}^2}\right)^{\frac{1}{\delta_{K_t}^2}} \frac{1}{\Gamma(1/\delta_{K_t}^2)} \left(\frac{k_t}{\underline{K}_t}\right)^{\frac{1}{\delta_{K_t}^2}-1} \exp\left(\frac{-k_t}{\delta_{K_t}^2 \underline{K}_t}\right), \tag{12}$$

where  $\delta_{K_t}$  is the dispersion parameter and  $\Gamma(z)$  is the gamma function defined for  $z > 0$ ,

$$\Gamma(z) = \int_0^{+\infty} t^{z-1} e^{-t} dt$$

There are limits for the dispersion parameter:

$$0 < \delta_{k_t} < \sqrt{1/3},$$

because the random variable  $K_t$  must be a second order random variable, i.e.,  $E\{K_t^2\} < +\infty$ .

To generate realizations of the random variable  $K_t$ , following the probability density function given by Eq. (12), the Matlab function GAMRND( $\alpha, \beta$ ) is used, where  $\alpha = 1/\delta_{K_t}^2$  and  $\beta = \underline{K}_t \delta_{K_t}^2$  are its corresponding parameters.

**Probabilistic Model for the Stiffness Matrix**

Now, the stiffness matrix, as a whole, is taken as uncertain. The goal is to discuss globally the uncertainties related to the modeling of the stiffness from the discretized system. A probability density function is constructed directly for the corresponding random matrix  $[\mathbf{K}]$ . This is done following the ideas described in Soize (2001, 2005).

As the goal here is to investigate the limits of the stochastic model, the matrix randomized is the one obtained by means of the FE discretization (instead of the reduced matrix). Matrix  $[\underline{\mathbf{K}}]$  is a positive-definite matrix and can be decomposed (Cholesky Decomposition) as in Eq.(13):

$$[\mathbf{K}] = [\underline{L}_K]^T [\underline{L}_K] \tag{13}$$

where  $[\underline{L}_K]$  is an upper triangular matrix.

Consequently, the random matrix  $[\mathbf{K}]$  can be written as in Eq. (14):

$$[\mathbf{K}] = [\underline{L}_K]^T [\mathbf{G}] [\underline{L}_K] \tag{14}$$

where  $[\mathbf{G}]$  is a random matrix such that: (1) it is positive-definite; (2) its expected value is the identity matrix, so  $E\{[\mathbf{G}]\} = [I]$ ; and (3)  $E\{\|[\mathbf{G}]^{-1}\|_F^2\} < +\infty$ , because writing Eq. (10) in the frequency domain, the corresponding stochastic equation has a unique second-order random solution if and only if  $E\{\|[\mathbf{K}]^{-1}\|_F^2\} < +\infty$ , where  $\|\cdot\|_F$  is the Frobenius norm,  $\|A\|_F = (tr[A]A^T)^{1/2}$ .

The probability density function of  $[\mathbf{G}]$  is constructed using the Maximum Entropy Principle and it is given by Eq. (15) (Soize, 2001):

$$p_{[\mathbf{G}]}([\mathbf{G}]) = 1_{M^+(R)}([\mathbf{G}]) C_G det([\mathbf{G}])^{(n+1)\frac{1-\delta^2}{2\delta^2}} \exp\left\{-\frac{(n+1)}{2\delta^2} tr[\mathbf{G}]\right\}, \tag{15}$$

where  $n$  is the dimension of the matrix  $[\mathbf{G}]$  and  $C_G$  is given by Eq. (16):

$$C_G = \frac{(2\pi)^{-n(n-1)/4} \left(\frac{n+1}{2\delta^2}\right)^{n(n+1)(2\delta^2)^{-1}}}{\left\{\prod_{j=1}^n \Gamma\left(\frac{n+1}{2\delta^2} + \frac{1-j}{2}\right)\right\}} \tag{16}$$

The dispersion parameter  $\delta$  is given by Eq. (17):

$$\delta = \left\{ \frac{1}{n} E\{\|[\mathbf{G}] - [I]\|_F^2\} \right\}^{\frac{1}{2}}, \tag{17}$$

and

$$0 < \delta < \left(\frac{n+1}{n+5}\right)^{1/2}.$$

The matrix  $[G]$  is built, for each realization of matrix  $[K]$ , decomposing (Cholesky decomposition)  $[G] : [G] = [L]^T [L]$ , where  $[L]$  is an upper triangular real positive-definite random matrix such that:

- The random variables  $\{[L]_{jj}, j \leq j'\}$  are independent.
- For  $j < j'$  the real-valued random variable  $[L]_{jj'} = \sigma V_{jj'}$ , in which  $\sigma = \delta(n+1)^{-1/2}$  and  $V_{jj'}$  is a real-valued Gaussian random variable with zero mean and unit variance.
- For  $j=j'$  the real-valued random variable  $[L]_{jj'} = \alpha(2V_j)^{1/2}$ , in which  $V_j$  is a real-valued gamma random variable with probability density function:

$$p_{V_j}(v) = \frac{1}{\Gamma\left(\frac{n+1}{2\delta^2} + \frac{1-j}{2}\right)} v^{\frac{n+1}{2\delta^2} - \frac{1+j}{2}} \exp(-v) \quad (18)$$

It can be noted that the random variables are generated by a normal distribution ( $V_{jj}, j \neq j'$ ) or by a gamma distribution ( $V_{jj}, j = j'$ ). Both of them are generated by Monte Carlo simulations using the Matlab, functions NORMRND(0,1) and GAMRND( $\alpha, \beta$ ), with  $\alpha = \left(\frac{n+1}{2\delta^2} + \frac{1-j}{2}\right)$  and  $\beta=1$ .

**Convergence of the Stochastic Solution**

Let  $[U(\theta, \omega)]$  be the response of the stochastic system calculated for a realization  $\theta$ , generated by the Monte Carlo method (Rubinstein, 1981). The mean-square convergence analysis with respect to independent realizations of the random variable  $\hat{U}$ , denoted by  $[\hat{U}_j(\theta, \omega)]$ , is carried out studying the function  $conv(n_s) \rightarrow conv(n_s)$  defined by

$$conv(n_s) = \frac{1}{n_s} \sum_{j=1}^{n_s} \int \|\hat{U}_j(\theta)\|^2 d\omega \quad (19)$$

For each realization  $\theta$ , the FRF  $H(\theta, \omega)$ , according to Eq. (8), is given by Eq. (20):

$$H(\theta, \omega) = \frac{\hat{U}_L(\theta, \omega)}{\hat{f}_L(\omega)} \quad (20)$$

As the goal is to compare the parametric and nonparametric probabilistic approaches, it is important to know the value of  $n_s$  (Eq. 19) beyond which the prescribed approximation is reached, that is, convergence is assured. This convergence analysis was performed for different values of the dispersion parameter and it was verified that the solution always converges for  $n_s = 500$ . Figure 4 shows an example for the function  $conv$ , considering the nonparametric approach, with  $\delta_{[K]} = 0.1$ .

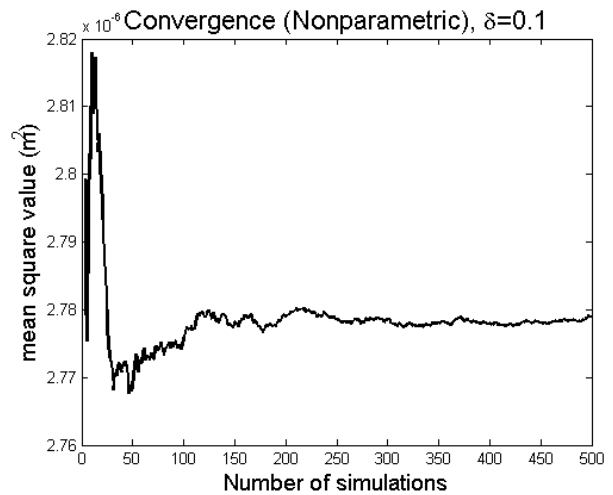


Figure 4. Convergence in the mean square sense.

**Numerical Simulations**

In order to better examine the results, fifty realizations of the random FRF  $H$  are shown in Fig. 5, using nonparametric approach, with  $\delta_{[K]} = 0.1$ .

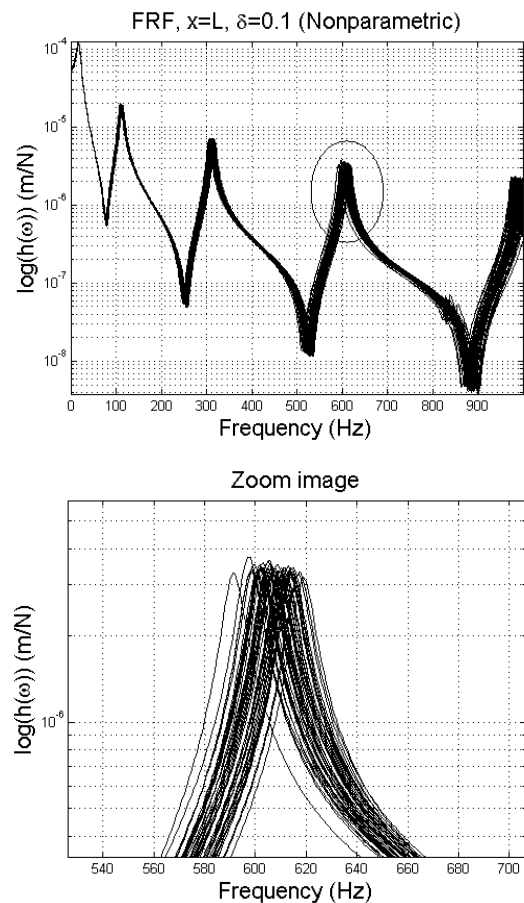


Figure 5. Fifty realizations of the FRF of using the nonparametric approach  $\delta_{[K]} = 0.1$  (top). Zoom image (bottom).

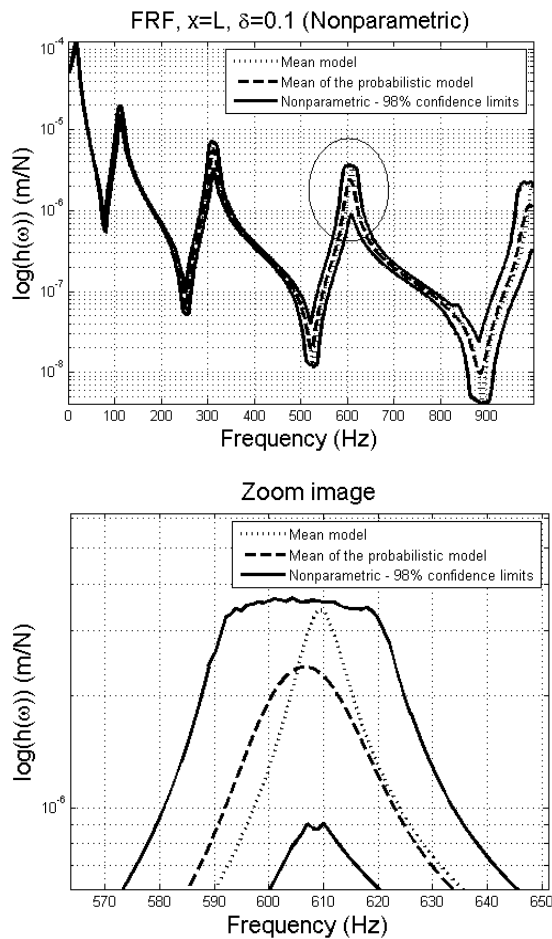


Figure 6. FRF of the mean model (dotted line), 98% confidence limits (solid lines) and the mean FRF using the nonparametric approach (dashed line),  $\delta_{K_I} = \delta_{K_J} = 0.1$  (top). Zoom image (bottom).

Figure 6 shows the response of the mean model and the mean response of the stochastic model. It should be noted that these two curves do not coincide. The thick lines represent the confidence region (Serfling, 1980) of 98% and it means that the response is inside the black envelope with probability 98%.

Some values of the coefficients of dispersion are chosen and confidence regions are constructed for the corresponding frequency response functions. Figure 7 shows confidence limits for both the parametric and nonparametric approaches, taking  $\delta_{K_I} = \delta_{K_J} = 0.1$ . Note that the confidence region is larger for the nonparametric approach and it includes the limits for the parametric approach. Also observe that, as the frequency increases, the confidence region becomes larger, showing the increase of the influence of uncertainties at high frequencies.

The coefficient of dispersion is then increased:  $\delta_{K_I} = \delta_{K_J} = 0.2$ . Figure 8 shows the confidence region of the FRFs obtained and also the corresponding FRF obtained for the mean model. It is also shown the corresponding FRF at  $x=L/2$ . Note that, in this case, the confidence region is larger. The limits for the nonparametric approach includes the limits for the parametric approach, and, as the frequency increases, the confidence region gets larger, as it was already pointed out in the previous case.

Figure 9 shows the results when the values of the coefficients of dispersion are taken at their greatest values, that is,

$$\delta_{K_I} = \frac{1}{3^{1/2}} \approx 0.58 \text{ and}$$

$$\delta_{K_J} = \frac{(49+1)^{1/2}}{(49+5)^{1/2}} \approx 0.96$$

In the top of Fig. 9, it is shown the confidence region for both parametric and nonparametric approaches, corresponding to the FRF. At the bottom of Fig. 9, the mean values for both probabilistic approaches are plotted. For the parametric approach, the behavior of the limits does not change much from what was seen in Figs. 7 and 8. However, for the nonparametric approach, we can note a different behavior. It happens because the sample space for the nonparametric approach is much larger than the sample space for the parametric approach, and the nonparametric approach is able to take into account model uncertainties, see Sampaio et al. (2007).

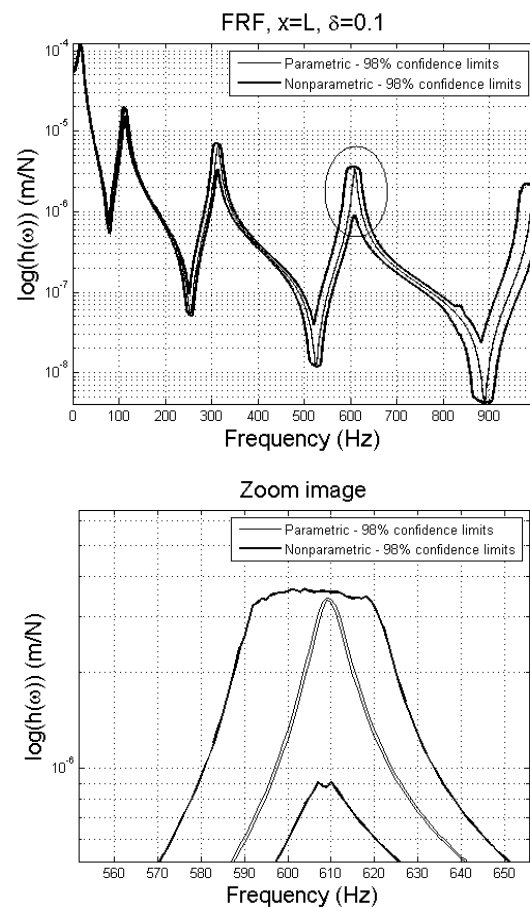


Figure 7. Envelope for a probability level of 98%, for both parametric and nonparametric probabilistic approaches, taking  $\delta_{K_I} = \delta_{K_J} = 0.1$  (top). Zoom image (bottom).

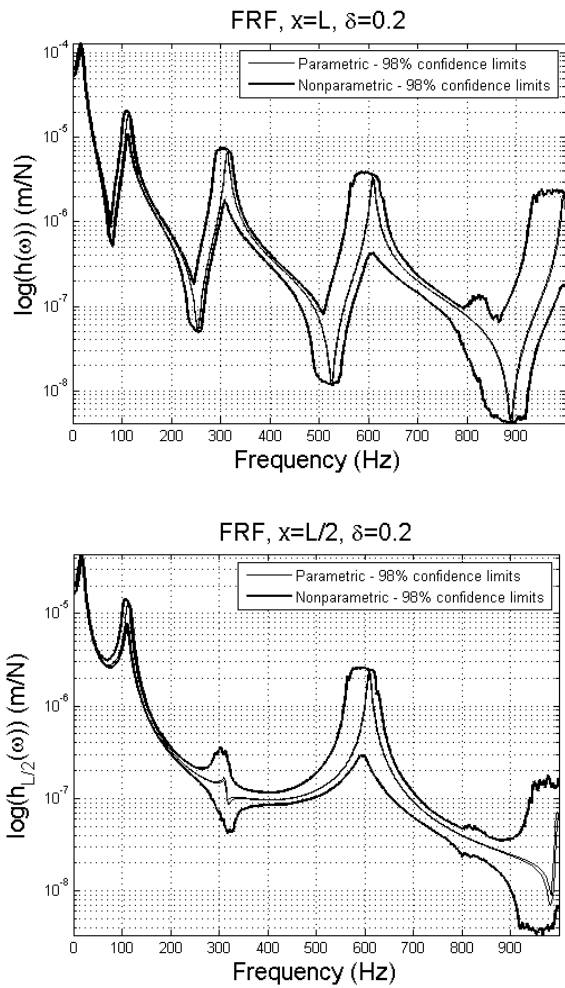


Figure 8. Confidence region for both parametric and nonparametric probabilistic approaches, taking  $\delta_{\kappa} = \delta_{\kappa I} = 0.2$ : response at  $x=L$  (top) and response at  $x=L/2$  (bottom).

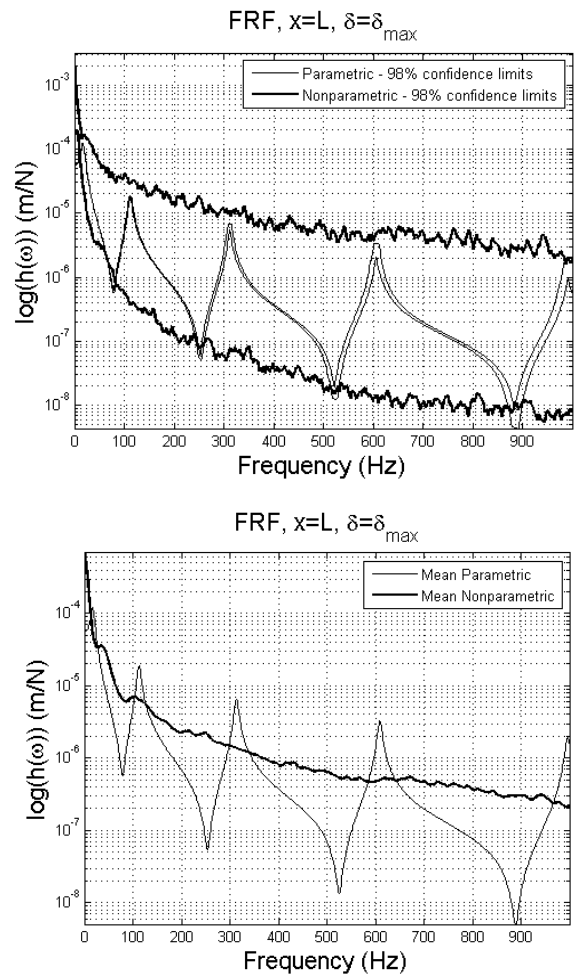


Figure 9. Confidence region for both parametric and nonparametric probabilistic approach with maximum values of the coefficients of dispersion:  $\delta_{\kappa} = 0.58$  and  $\delta_{\kappa I} = 0.96$  (top) and expected values for the FRFs, with maxima values of the coefficients of dispersion:  $\delta_{\kappa} = 0.58$  and  $\delta_{\kappa I} = 0.96$  (bottom).

### Model Uncertainties

The nonparametric approach can be used to take into account model uncertainties (Soize, 2001, 2005; Sampaio et al., 2007), including boundary conditions uncertainties. To show how the methodology works, three different (deterministic) boundary conditions are considered and their results compared with those previously obtained with the stochastic system discussed.

Clearly, the idea is to discuss uncertainties present in a model, and it is not to change completely the model. However, it is important to investigate the limits of the nonparametric approach in predicting possible responses of a system.

The three cases considered are (Fig. 10):

1. Essential boundary conditions at  $x = 0 : u_a|_{x=0} = 0$  and  $u_v|_{x=0} = 0$ ;
2. Essential boundary conditions at  $x = 0 : u_a|_{x=0} = 0$ ,  $u_v|_{x=0} = 0$  and  $u_r|_{x=0} = 0$ ;
3. Essential boundary conditions at  $x = L : u_a|_{x=L} = 0$  and  $u_r|_{x=L} = 0$ ;

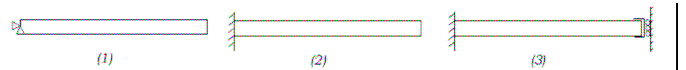


Figure 10. Boundary conditions for cases (1), (2) and (3).

It should be noted that matrix  $[K]$  will have different dimensions for each case because of the restricted degrees of freedom, but the dimension does not affect the analysis.

There is no uncertainty in cases (1), (2), and (3); and they have clearly different responses, as shown in Fig. 11.

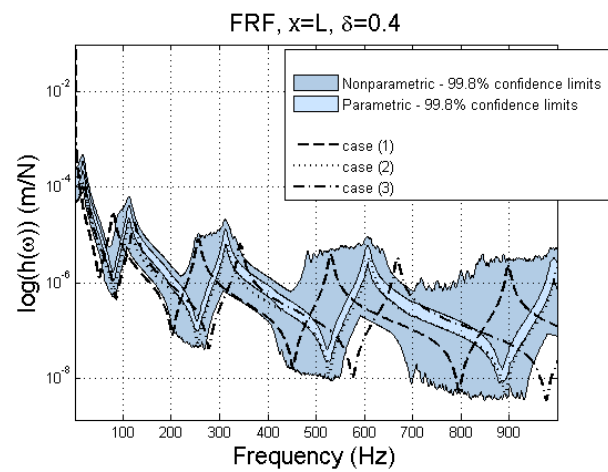
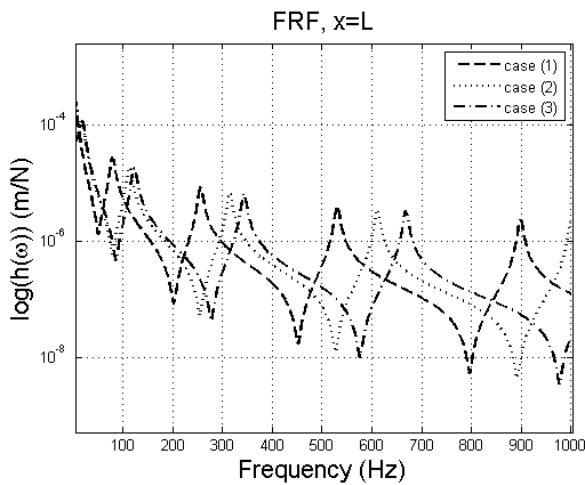


Figure 11. FRFs for three deterministic cases: (1)  $k_t = 0$ , (2) clamped-free and (3) clamped-locked.

Figure 12 shows the FRFs for the three cases of boundary conditions together with the confidence limits of the probabilistic parametric and nonparametric approaches previously discussed. On the top of Fig. 12, the values of the coefficient of dispersion are taken as 0.4, in both parametric and nonparametric approaches, and at the bottom of Fig. 12, the values of the coefficient of dispersion are taken as their greatest values.

In both plots (top and bottom) we note that the limits for the parametric approach are far away from the response perceived. However, this does not happen when the nonparametric approach is considered. For a coefficient of dispersion of 0.4, the confidence region almost includes the three responses of the deterministic problems simulated. It does not mean that the result is satisfactory, indeed it is not. When the value of the coefficient of dispersion is greatest, the limits are so wide that all possible responses may occur.

The confidence region for the parametric approach is very thin and therefore this methodology is very efficient if the source of uncertainty is concentrated in the clamped boundary condition. We should understand our system so that we can estimate where the biggest sources of uncertainties are located. If we have a good model and we know where the sources of uncertainties are concentrated, the parametric stochastic approach is the best one. However, there are cases where: (1) the model used is simplified because to use a more detailed model is very time consuming, (2) the equations to the problem are not well established so we are not sure about the best model, (3) the system changes with the production process that changes with time, (4) system responses have large dispersions etc. In these situations the best we can do is to use the nonparametric probabilistic approach to allow for cases that our model cannot predict. But note that the value of  $\delta_{[K]}$  can not be adjusted a priori so that the experimental results fit in the confidence region. The dispersion parameter  $\delta_{[K]}$  has to be determined experimentally.

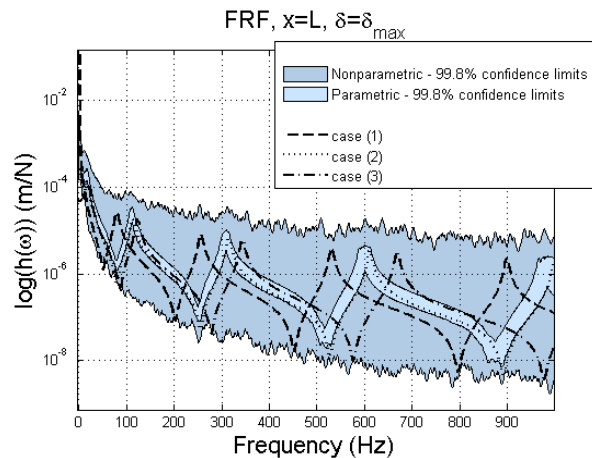


Figure 12. FRFs for three deterministic cases: (1)  $k_t = 0$ , (2) clamped-free and (3) clamped-locked, together with the confidence limits for parametric and nonparametric approaches with probability level of 99.8%.  $\delta_{\alpha} = \delta_{\kappa} = 0.4$  (top) and maximum values  $\delta_{\alpha} = 0.58$  and  $\delta_{\kappa} = 0.96$  (bottom).

### Concluding Remarks

A Timoshenko beam with uncertain boundary conditions was analyzed in order to discuss uncertainties on the boundary conditions. First, the stiffness of a torsional spring inserted in one end of the beam was modeled as uncertain. Then, the stiffness matrix was modeled as uncertain. Each one of the approaches led to different results. Considering the same coefficients of dispersion, the confidence region of the response for the nonparametric approach was larger than the confidence region for the parametric approach. As an application, different boundary conditions were considered for the same beam and the resulting systems were analyzed.

Concerning the differences between the two approaches used, some points should be remarked:

- The numerical simulations showed that, for the problem analyzed and using a 98% confidence limit, the nonparametric approach includes the parametric approach. Indeed, the possible outcomes of the nonparametric approach lies in a larger sample space than the possible outcomes of the parametric approach.
- In the parametric approach only one entry of matrix  $[K]$  is random while in the nonparametric approach the whole matrix  $[K]$  is random.
- The sample space is one-dimensional manifold for the parametric approach while for the nonparametric approach the



sample space is multi-dimensional (the dimension depends on the size of  $[\mathbf{K}]$ ).

- It is possible to take into account model uncertainties with the nonparametric approach, but with the parametric approach it is not possible.
- The dispersion parameter of matrix  $[\mathbf{K}]$ ,  $\delta_{[\mathbf{K}]}$ , has to be determined experimentally or else it can be adjusted to include any response, diminishing the predictability of the model.
- For both approaches, as the frequency increases, the predictability decreases. So, we must be careful when analyzing high frequency problems.

If we have information about the source of uncertainty, this information should be used to improve the predictability of the system. We are dealing with a case where the uncertainty is in the model, more precisely, in the boundary conditions. This information allowed us to create a model to the clamped boundary condition so that the parametric probabilistic approach could be used. The nonparametric probabilistic approach should be used for generalized uncertainties, because if the uncertainty is localized (as in boundary conditions), the realizations of the model may lead to cases that do not correspond to the physics of the problem studied.

### Acknowledgements

The authors acknowledge the financial support of CNPQ, CAPES, and FAPERJ.

### References

- Bazoune, A. and Khulief, Y.A., 2002, "Shape functions of the three-dimensional Timoshenko beam element", *Journal of Sound and Vibration*, 259(2), pp. 473–480.
- Cataldo, E., Sampaio, R., Lucero, J. and Soize, C., 2008, "Modeling random uncertainties in voice production using a parametric approach", *Mechanics Research Communications*, 35(7), pp. 454–459.
- Cataldo, E., Soize, C., Desceliers, C. and Sampaio, R., 2007, "Uncertainties in mechanical models of larynx and vocal tract for voice production", Proceedings of the XII DINAME, Ilhabela, SP.
- Cataldo, E., Soize, C., Sampaio, R., Desceliers, C., 2009, "Probabilistic modeling of a nonlinear dynamical system used for producing voice", *Computational Mechanics*, 43(2), pp. 262–275.
- Ewins, D.J., 1984, "Modal Testing: Theory and Practice", John Wiley & Sons Inc., Hoboken, New Jersey.
- Inman, D.J., 2007, "Engineering Vibration", Prentice-Hall, Inc., Upper Saddle River, N.J. USA, 3<sup>rd</sup> edition.
- Jaynes, E., 1957a, "Information theory and statistical mechanics", *The Physical Review*, 106(4), pp.1620–630.
- Jaynes, E., 1957b, "Information theory and statistical mechanics ii", *The Physical Review*, 108, pp.171–190.
- Kapur, J.N. and Kesavan, H.K., 1992, "Entropy Optimization Principles with Applications", Academic Press, Inc., USA.
- Nelson, H.D., 1980, "A finite rotating shaft element using Timoshenko beam theory", *Journal of Mechanical Design*, 102, pp. 793–803.
- Reddy, J.N., 2005, "An Introduction to the Finite Element Method", McGraw-Hill.
- Ritto, T.G., Aguiar, R., Sampaio, R. and Cataldo, E., 2008, "How to match theoretical and experimental boundary conditions of a cantilever beam", Proceedings of the 7th European Conference on Structural Dynamics E110, EURO DYN.
- Rubinstein, R.Y., 1981, "Simulation and the Monte Carlo Method", John Wiley and Sons.
- Sampaio, R. and Ritto, T.G., 2008, "Short course on dynamics of flexible structures – deterministic and stochastic analysis", Seminar on Uncertainty Quantification and Stochastic Modeling, PUC-Rio, September.
- Sampaio, R., Ritto, T.G., and Cataldo, E., 2007, "Comparison and evaluation of two approaches of uncertainty modeling in dynamical systems", Mecánica computacional, ENIEF, Córdoba, Argentina, Vol. XXVI, pp. 3078–3094.
- Sampaio, R. and Soize, C., 2007, "On measures of nonlinearity effects for uncertain dynamical systems application to a vibro-impact system", *Journal of Sound and Vibration*, 303, pp. 659–674.
- Serfling, R.J., 1980, "Approximation Theorems of Mathematical Statistics", JohnWiley and Sons, USA.
- Shannon, C.E., 1948, "A mathematical theory of communication", *Bell System Tech. J.*, 27, pp. 379–423 and pp. 623–659.
- Soize, C., 2001, "Maximum entropy approach for modeling random uncertainties in transient elastodynamics", *Journal of the Acoustical Society of America*, 109(5), pp.1979–1996.
- Soize, C., 2005, "A comprehensive overview of a non-parametric probabilistic approach of model uncertainties for predictive models in structural dynamics", *Journal of Sound and Vibration*, 288(3), pp. 623–652.
- Soize, C., 2008, "Short course on uncertainties and stochastic modeling", Seminar on Uncertainties and Stochastic Modeling, PUC-Rio, August.